Modeling of Internal Defects in Logs for value Optimization based on Industrial CT Scanning

Jean-Philippe Andreu, Alfred Rinnhofer
Institute for Digital Image Processing
JOANNEUM RESEARCH,
Wastiangasse 6, A-8010 Graz, Austria
email: [jean-philippe.andreu, alfred.rinnhofer]@joanneum.at

Abstract

For spruce (*Picea abies* (L.) Karst.), as with most other species, the value of a log is to great extent determined by its defects. That is the reason why sawyers, aiming at the optimal utilization of a log, were naturally interested in defects, their number, position and shape. X-ray computer tomography (CT) scanning is able to detect internal density variations related to defects. In order to use this information for optimizing a computer based sawing process, it is necessary to model different defects by geometric descriptions which are easy to handle. This study describes how to detect and model internal wood defects like pith, cracks, knots and resin pockets in spruce logs from non-destructive measurements using industrial CT and automatic image analysis processes. The proposed methods and models are experimentally evaluated by destructive measurements.

1. Introduction

Internal defects ultimately determine the value of a log for the lumber industry. It has been shown that acquiring a detailed knowledge of the location and size of internal defects prior to the first cut into the log is estimated to lead to potential gains in lumber value [7].

1.1 Industrial CT Scanning

For about 20 years, research has been conducted to find non-destructive technologies to scan logs for internal defects. Along with other techniques using Gamma rays, nuclear magnetic resonance, microwaves, ultrasounds, vibrations, longitudinal stress waves, X-ray technology was identified as one of the most promising technology to image the internal structure of logs. Good overviews and descriptions of these different technologies can be found in [5, 15]. Because of similar density ranges between human tissues and wood, X-ray technologies (including CT) have been the most widely investigated techniques for scanning wood.

CT technology was first introduced for medical purposes in 1972. So naturally, early log scanning research started with medical scanners. Even though medical CT scanners have proven their ability to produce images of really high quality, trials using medical CT scanners for scanning logs have been limited to small logs. Medical CT scanners have, by design, strict limits (in terms of duty cycle, speed and gantry size) which are hindering these machines to scan normal sized logs all day long within the harsh industrial environment of a sawmill. CT scanners developed for airport security purposes (metal and explosive detection) have bridged the gap between the medical and the industrial CT application domains. These scanners [14] work like their medical cousins but their x-ray systems are designed for operating at a duty cycle of 100% 24 hours a day. They allow a bigger gantry than medical CT scanners and can be operated at a higher speed. But such changes in design result in a lower image quality compared with what medical CT scanners can provide.

1.2 Related work

Modeling defects like knots is critical to any cut optimization process (search of an optimal cut solution) which can have difficulties in handling huge amount of data. Reconstruction of a 3D object model from real-world measurements aims at encapsulating the shape of a 3D object into a parametrical mathematical formulation. Parametric descriptions dramatically reduce the amount of data (i.e. measurements) to handle, translate the 3D objects into a continuous function while keeping the representation detailed. While most of the researchers put effort on precisely classifying pixels either as defect (belonging to a specific defect type such as knot, void, rot, etc...) or non-defect, less effort was put in designing models for wood defects.

The pith is usually modeled as the center of the tree growth rings. Several attempts in detecting annual rings and localizing the pith have been investigated [3, 11]. Since annual rings are a succession of small ridge and valley structures efficient techniques for detecting them should accommodate to the image quality of industrial CT scanners. Unfortunately none of techniques known to the authors displayed adaptiveness to the image quality.

J.E. Aune [2] and M. Samson [13] developed geometrical models to describe knots within logs. Grundberg [5] developed a model for Scots pine knots. This model describes a knot as three functions (knot diameter, tangential and longitudinal position) of the radial distance to the pith. This model can not describe the longitudinal position of knots changing direction from upwards to downwards since the function used for modeling the longitudinal position is an increasing function. Oja [10] later improved this model for Norway spruce by using a complicated non-linear function (a mixture of *ln(x)* and *tan(x)*) for describing the longitudinal position of the knots and finally concluded that there is no significant difference in accuracy between his model and the one developed by Grundberg.

2. Pith Detection

Spruce logs were scanned using an Invision CTX 2500 CT scanner with a pixel resolution of 1.55 mm by 1.55 mm, an intensity resolution of 12 bits per pixel (i.e. 4096 gray levels) and an image size of 512x512 pixels. An image was taken every 20 mm with a scanning transversal feeding speed of 1.5 m/min.

2.1 Annual ring Enhancement

A CT image displaying annual rings can be viewed as an image of oriented textures. In a local neighborhood where no defect (cracks, knots, etc...) appear, the gray levels along ridges and valleys can be modeled as a sinusoidal-shaped wave along a direction (see Fig. 1).

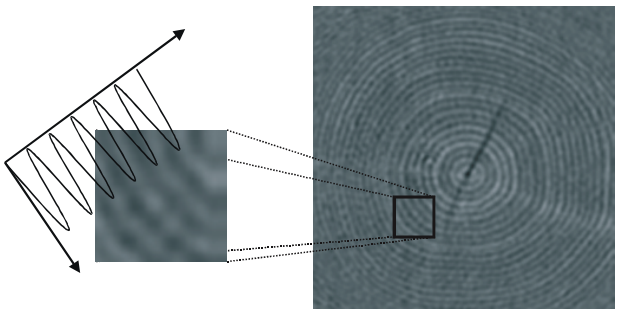

Fig. 1. Local oriented sinusoidal-shaped wave.

The structure of parallel ridges and valleys with well defined frequency and orientation provides useful information for removing noise. Sinusoidal-shaped waves of ridges and valleys vary slowly in frequency and keep a local constant orientation. A bandpass filter that is tuned to the corresponding frequency and orientation can efficiently remove noise while preserving the ridge/valley structure. Gabor filters are both frequency and orientation dependent and have optimal joint resolution in both spatial and frequency domain [8].

The following figure (Fig.2) displays the difference between a global "hand-tuned" bandpass filter (Fig.2 middle) and automatically tuned local Gabor filters.

Fig. 2. Enhancement: Original image (left), hand-tuned bandpass filter (middle), automatically tuned local Gabor filters (right).

The improvement is clearly visible. The adaptive behavior of our algorithm helps in restoring annual rings in really bad quality portions of the image (e.g. the image corners) where the annual rings are difficult to distinguish even to human eyes. Even the crack is suppressed due to the low frequency of the pattern. Still some imperfections remain near to the pith because of the high curvature (in comparison to the size of the local neighborhood) of the annual rings at this position.

2.2 Pith Localization

We localize the pith by considering it as the center of the concentric annual rings. The annual rings are obtained by simply thresholding the enhanced image.

One of the most popular method for detecting shapes like circle in an image is the Hough Transform [9] (HT). The HT is robust to noise, shape distortions and occlusions. Its main disadvantage is that computational and storage requirements of the algorithm increase as a power of the dimensionality of the curve to be recognized. To overcome this dimensionality the search space should be decomposed. Usually a HT for circle detection decomposes the three dimensional search in a two dimensional HT for detecting circle centers followed by a one dimensional radius histogram search for determining the radius values. If we suppose annual rings to be concentric circles only the first step (detecting circle centers) of the transformation is needed for localizing the pith.

The two dimensional HT for detecting circle centers takes place into a discrete space (usually called "parameter space") whose points are candidates for being the center of a circle. Since we defined the pith as the center of all annual rings (themselves modeled as concentric circles), the point with the most votes in the parameter space (maximum) gives the position of the pith (see Fig. 3).

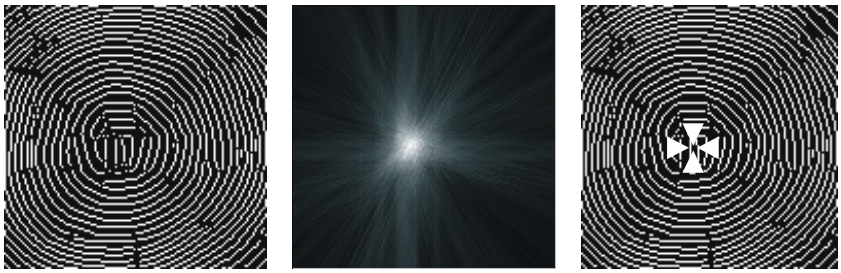

Fig. 3. Pith Localization: Annual rings (left), HT parameter space (center), pith as maximum of the parameter space (right).

3. Crack Detection

A crack is a separation of wood due to the tearing apart of cells, appearing in logs when they start to dry. There are mainly two types of cracks: radial and longitudinal. The first ones are perpendicular to the annual rings and usually go through the pith; the second ones are parallel to the annual rings.

3.1 Crack Segmentation

Due to both the thin shape of cracks and the presence of noise in the industrial CT images simply applying a global threshold does not suffice for segmenting the cracks. Radial cracks, together with knots are defects originating from the pith and having a radial direction. After detecting the pith we apply directional filters enhancing cracks and reducing other non-radial wood defects like the annual rings and the resin pockets. We actually use a bank of 12 directional filters whose results are combined in order to recover the most useful information. Figure 4 shows the result of the application of two of the directional filters of the filter bank. One of the filter enhances structures having a horizontal orientation (Fig.4 middle) while the other enhances vertically oriented structures (Fig.4 right). In the last case it can be clearly seen that the crack is well preserved while the annual rings are removed.

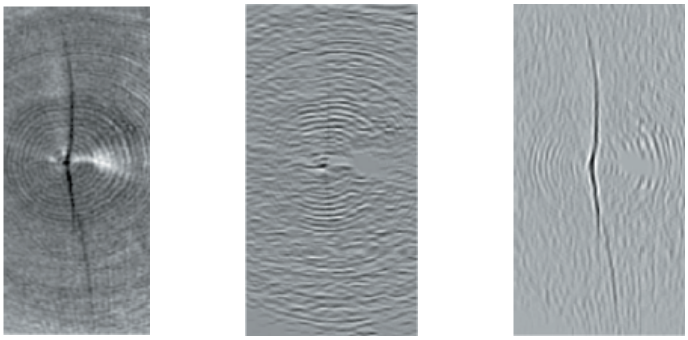

Fig. 4: Crack Detection: original image (left), horizontal filter (middle), vertical filter (right).

Once the results of the different filters are combined, the cracks are then segmented by adaptive thresholding.

3.2 Crack Modeling

Cracks in CT images can be simplified by line segments without much loss of information. Since cracks are defects with a certain extend along the log length, cracks appearing in successive CT images give support for modeling a crack in 3D. Cracks in successive CT images are grouped together depending on their position and direction with respect to the pith. Delaunay triangulations [6] can be used to build topological structures from unorganized (or unstructured) points. Representing cracks as 3D meshes is convenient for 3D graphics rendering but also for the computation of their intersection with cutting (sawing) planes. Figure 5 (right) shows a rendered model of a crack computed from a sequence of images (Fig. 5 left).

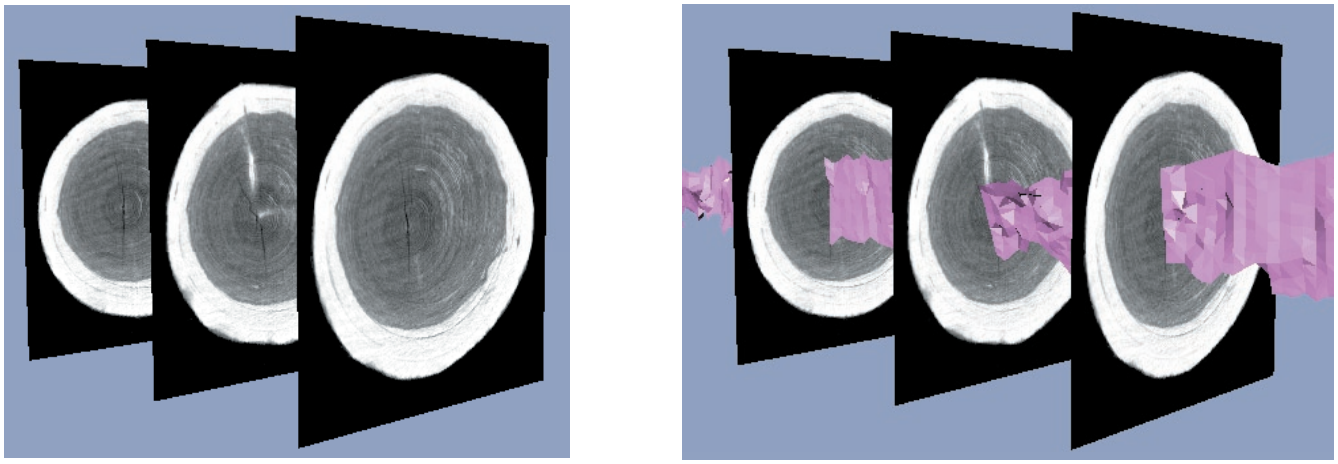

Fig. 5: Crack Modeling: CT image sequence (left), rendered crack (left)

4. Knot Detection

Knots are portion of branches that are embedded in the wood of a tree trunk.

4.1 Knot Modeling

On account of their material density which is higher than its surrounding, knots can be characterized by high CT values in the images. To segment the knots from their surrounding we use a multi-modal histogram thresholding technique [4] after several image pre-processing steps (i.e. remove the annual rings, segment the sapwood, etc.).

4.2 Knot Modeling

Knots detected in successive CT images can be grouped together in order to model a knot in 3D. The grouping is performed on the distance of the knots to the pith and on the direction of their principal axis in the CT image plane. Each group representing a series of 2D regions that are spatially connected across CT images is then modeled as a single knot in 3D. Note that some knots are lacking of 3D support (e.g. knots only appearing on a single CT image). Each knot is mathematically modeled by a curve in 3D (spine) along which a 2D cross-section (a planar patch) is swept. Ideally the sweeping of a 2D shape along a path in 3D creates a volume (swept volume or generalized cylinder). The shape of the 2D cross-section is fixed but can be differently scaled at each point of the spine. If the function representing the spine lays on a plane, each knot is having a symmetry plane and the spine

function can be describe as a 2D function within this symmetry plane. The origin of the spine function is located at the pith of the CT image where the knot first appeared. The knot symmetry plane is perpendicular to the CT image plane, passes through the pith and has an angle α with the CT image plane.

This mathematical model matches the VRML97 extrusions [16]. VRML extrusions are based on a two dimensional cross-section extruded along a three dimensional spine. The only difference between our knot model and a VRML extrusion lays in the piecewise linearity of the 2D cross-section and the 3D spine of the VRML shape. Using these VRML extrusions prove convenient not only for 3D graphics rendering but also for fast computation, with the help of computational geometry algorithms, of the intersection of these shapes with cutting planes. The following figure (Fig.6) shows a rendered model (textured and wire-framed) of a knot where all the information necessary to the modeling are depicted:

- The knot symmetry plane (outlined in gray)
- The scale function of the 2D cross-section
- The angular position of the symmetry plane with respect to the CT image plane
- The planar spine function
- The pith position in the CT image

The model we use for spruce describes a knot by four parameters. These parameters do not include the three parameters defining the origin of the knot. For the 2D cross-section we simply use a circle.

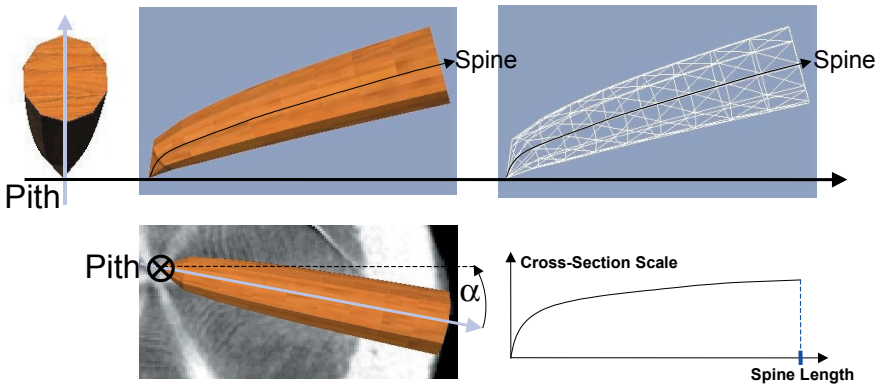

Fig. 6: Knot Model description.

One parameter α defines the angle between the symmetry plane and the image plane.
Two parameters describe the planar (in the knot symmetry plane) spine function:

$$Spine(r) = a\sqrt{r} + br,\ r \in [0, KnotLength] \rightarrow [0, KnotHeight] \quad (1)$$

One parameter models the scale function of the 2D circular cross-section:

$$Scale(r) = c\ln(r+1),\ r \in [0, KnotLength] \rightarrow [0, KnotMaxDia\ meter] \quad (2)$$

In the equations (1) and (2), the variable r defines the radial distance from the pith.

The following figure (Fig. 7) shows a 3D rendering of knot models within a log. The models were computed from automatically detected knots in successive CT images of log scan.

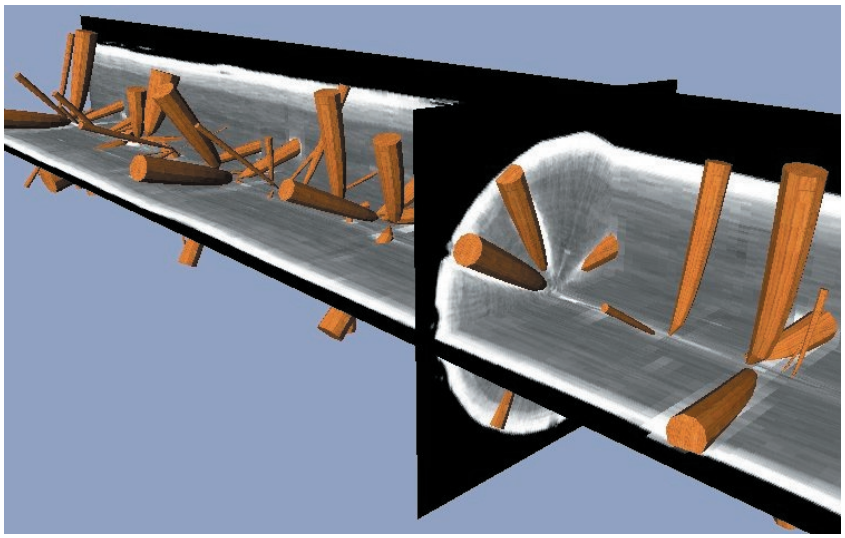

Fig. 7: Knot Models rendered within a log.

5. Resin Pocket Detection

Resin pockets are lens-shaped accumulations of resin or solidified resin. How to detect and model this type of defect will not discussed in this paper but the reader can refer to [12] for a detailed explanation as well as an experimental evaluation of the processes.

6. Experimental Evaluation

We describe in this section an experimental evaluation of our methods for detecting and modeling defects. We only present here the performance of the pith and knot detection while the evaluation for resin pockets could be found in [12]. Measuring the performance of the crack detection is a problematic task because cracks open up or close down when boards are sawed meaning that ground truth data are difficult to gather for this type of defect. This will be addressed in future work.

6.1 Pith

The performance of the pith localization is shown in Figure 8. Roughly 270 CT images of a rather bent log (to get noticeable variations in pith coordinates) were computed and the results were compared to the exact position of the pith within each image. Since the three dimensional position of the pith cannot be displayed, we just show the variations of the pith X and Y coordinates (in the CT image coordinate system) along the log.

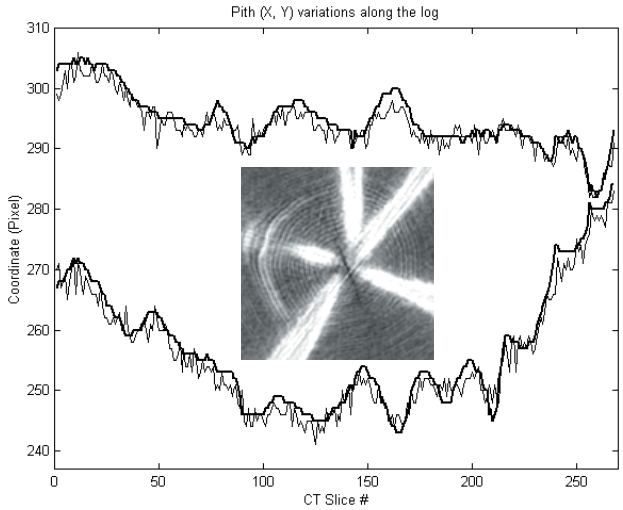

Fig. 8: Pith localization evaluation: exact position (bold curves) compared with automatically processed localization (thin curves). Middle: CT image where the localization error is maximum.

We can see that the coordinates X and Y of the pith (bold curves on Fig.8) do not vary smoothly along the log thus making interpolation techniques difficult. In comparison automatically processed localization curves looks ”jaggy” (the thin curves on Fig.8) but still stick to the true data. These variations are partially explained by the fact that defects (principally knots) reduce the amount of annual rings in the image and thus lower the efficiency of our algorithm. Another source of inaccuracy comes from the assumption that the annual rings are concentric. This does not always hold even though the nearer we are to the pith the less eccentric the annual rings are. So there is a trade-off: the more annual rings considered the more precise the localization but the more sensitive to eccentricity.

However on this example, the distance error between true data and computed ones has a mean of 2.2 pixels with a low standard deviation of 1.2 pixels while reaching a maximum of 6.7 pixels. Local post processing like smoothing might even decrease this error rate. The image on Figure 7 displays where the error is maximum (note the knots disturbing the annual ring patterns).

6.2 Knots

The procedures for detecting and modeling the knots described in section 4 were experimentally validated on four logs, two of them having knots changing direction from upwards to downwards. The logs were scanned and then cut into 23mm parallel boards. The boards were then imaged with an optical line scan camera with a pixel resolution of 1mm by 1mm. The position and the maximum diameter of the knots appearing on the board faces were manually recorded and treated as ground truth. After detecting and modeling the 3D knots out of the CT data their intersection with the cutting plane corresponding to each board face was automatically computed. For visual control and validation purposes the intersections between the 3D knots and the cutting planes were then overlaid onto the scanned images of the board faces. The following figure (Fig. 9) depicts a part of a scanned knotty board where its intersection with the 3D knots have been overlaid.

Fig. 9: Part of an optically scanned board with knots and detected knots overlaid

The detection rate and false alarm rate were then computed. The detection rate is defined as the ratio of the number of true knots detected to the total number of true knots appearing on the board faces. The false alarm rate is defined as the ratio of the number of false knots detected to the total number of knots detected (true and false knots).

The detection and false alarm rates for knots having a diameter of at least 10mm averaged to 96% and 10% respectively. If all knots were considered, the detection rate falls to 73% and the false alarm rate reaches 13%. The following table (Table 1) shows the accuracy of the knot modeling with respect to the knot size and position.

Table 1: Knot model accuracy for knots whose diameter > 10mm

Knot Parameter	Mean Value	Standard Deviation
Angular position: α	1.9°	2.9°
Elevation position	0.9 mm	10.4 mm
Diameter	0.7 mm	10.1 mm

7. Conclusion

We have shown how to detect and model defects for Norway spruce from industrial CT images using automatic image analysis algorithms. Results showed both a good detection rate and a satisfactory model accuracy even though the present industrial scanner system we used has limitations in term of resolution and speed.

The spatial resolution of the scanner in the CT image plane is fixed by mechanical constraints (number of sensors on the detector array, sensor size, focus size on the anode, gantry diameter, etc.) while the resolution in the direction perpendicular to the CT plane is mainly fixed by the feeding speed of the scanner: the quicker the speed the lower the contrast (averaging effect). An image was taken every 20 mm with a speed of 1.5 m/min. Practically this is too slow for volume oriented high-speed sawmills, but sufficient for quality oriented sawmills. Limitations also came from the data acquisition. The whole spiral was not completely taken into account by the reconstruction algorithm resulting in "gaps" within the data.

However the resolution of industrial CT scanners seems to be a viable solution for internal CT log scanning. Their resolution gives most of the necessary information for log grading thus giving high expectations (especially if new generations of industrial CT scanners overcome the mentioned limitations) for a fully automated system where defect identification and log breakdown optimization would be done by computers, using all available information about the inner structure of the log.

References

[1] Andreu J.Ph. and Rinnhofer A.: “Enhancement of annual rings on industrial CT images of logs”, Proc. ICPR2002, Vol. III (2002), 261-264.

[2] Aune J.: “An X-ray Log-Scanner for Sawmills”, Proc. Of the 2nd Int. Workshop on Scanning Technology and Image Processing on Wood (1995), 51-65.

[3] Chalifour A., Nouboud F., Deprost B. and Okana S.: “Automatic Detection of Tree-Rings on Wood Disc Images”, Proc. QCAV2001 (2001), 348-352.

[4] Chang J.H., Fan K.C. and Chang Y.L.: “Multi-modal gray-level Histogram Modeling and Decomposition”, Image and Vision Computing, vol. 20 (2002), 203-216.

[5] Grundberg S.: “Scanning for internal defects in logs”, Ph.D. thesis, Lulea Univ. of Tech., (1994) ISSN 0280-8242.

[6] Gudmundsson J., Hammar M. and Van Kreveld M.: “Higher order Delaunay triangulations”, Computational Geometry, vol. 23, no. 1 (2002), 85-98.

[7] Hodges D.G., Anderson W.C. and Mac Millin C.W.: “The economic potential of CT scanners for hardwood sawmills”, Forest Products Journal 40, vol. 3 (1990), 65-69.

[8] Jain A.K. and Farrokhnia F.: “Unsupervised Texture segmentation using Gabor Filters”, Pattern Recognition, vol. 24, no. 12 (1991), 1167-1186.

[9] Leavers V.F.: “Which hough transform?”, CVGIP - Image Understanding, vol. 58, no. 2, no. 2 (1993), 250-264.

[10] Oja J.: “X-ray Measurement of Properties of Saw Logs”, Ph.D. thesis, Lulea Univ. of Tech., (1999) ISSN 1402-1544.

[11] Onoe M., Tsao J.W., Yamada H., Nakamura H., Kogura J., Kawamura H. and Yoshimatsu M.: “Computed tomography for measuring the annual rings of a live tree”, Nuclear instruments and methods in physics research, vol. 221, no. 1 (1984), 213-220.

[12] Parziale G.: “Detecting Resin Pockets in CT Images with Anisotropic Diffusion Filtering”, Proc. of the 5th International Conference on Image Processing and Scanning of Wood, (2003)

[13] Samson M.: “Modeling of knots in logs”, Wood Science and Tech., vol. 27 (1993), 429-437.

[14] Schmoldt D.L., Scheinman E., Rinnhofer A. and Occeña L.G.: “Internal log scanning: Research to reality”, Proc. of the Hardwood Research Council Meeting, (2000)

[15] Skatter S.: “Non destructive determination of the external shape and the internal structure of logs-Possible technologies for use in the sawmills”, Ph.D. thesis, Agricultural Univ. of Norway, ISBN 82-575-0352-5 (1998)

[16] VRML97, The Virtual Reality Modeling Language, http://www.web3d.org/Specifications/